

1 **Spectroscopic and Quartz Crystal Microbalance (QCM) Characterization of Protein-**
2 **based MIPs**

3

4 Hazim F. EL-Sharif¹, **Hiddenbou Aizawa²**, Subrayal M. Reddy^{1*}

5

6 ¹Department of Chemistry, Faculty of Engineering and Physical Sciences, University of
7 Surrey, Guildford, Surrey, GU2 7XH, UK

8 ²**Institute for Environmental Management Technology, National Institute of Advanced**
9 **Industrial Science and Technology (AIST), 1-1 Higashi, Tsukuba 305-8565, Japan**

10

11 ***Corresponding Author**

12 Tel : +44 (0) 1483686396, s.reddy@surrey.ac.uk

13

14 **Abstract**

15 We have studied acrylamide-based polymers of varying hydrophobicity (acrylamide, AA; N-
16 hydroxymethylacrylamide, NHMA; N-isopropylacrylamide, NiPAm) for their capability of
17 imprinting protein. Rebinding capacities (Q) from spectroscopic studies were highest for
18 bovine haemoglobin (BHb) MIPs based on AA, $Q = 4.8 \pm 0.21 < NHMA, Q = 4.3 \pm 0.32 <$
19 $NiPAm, Q = 3.6 \pm 0.45$, while also demonstrating low selectivities for non-template proteins
20 ($<30 \pm 5\%$), with the exception of bovine serum albumin (BSA, $>76 \pm 0.5\%$). When applied
21 to the QCM sensor as thin-film MIPs, NHMA MIPs were found to exhibit best discrimination
22 between MIP and non-imprinted control polymer (NIP) in the order of $NiPAm < AA <$

23 NHMA. The extent of template removal and rebinding, using both crystal impedance and
24 frequency measurements, demonstrated that 10% (w/v):10% (v/v) sodium dodecyl
25 sulphate:acetic acid (pH 2.8) was efficient at eluting template BHb (with $80 \pm 10\%$ removal).
26 Selectivity studies of NHMA BHb-MIPs revealed higher adsorption and selective recognition
27 properties to BHb (64.5 kDa) when compared to non-cognate BSA (66 kDa), myoglobin
28 (Mb, 17.5 kDa), lysozyme (Lyz, 14.7 kDa) thaumatin (Thau, 22 kDa) and trypsin (Tryp, 22.3
29 kDa). The QCM gave frequency shifts of $\sim 1500 \pm 50$ Hz for template BHb rebinding in both
30 AA and NHMA MIPs, whereas AA-based MIPs exhibited an interference signal of $\sim 2200 \pm$
31 50 Hz for non-cognate BSA in comparison to a $\sim 500 \pm 50$ Hz shift with NHMA MIPs. Our
32 results show that NHMA-based hydrogel MIP are superior to AA and NIPAM..

33

34 **Keywords:** Molecular imprinted polymer (MIP); Hydrogel; Protein; Biosensor; QCM

35 **1. Introduction**

36 1. Introduction

37 In recent years, molecularly imprinted polymers (MIPs) have allowed selective extractions
38 that rival immunoaffinity-based separations, and have shown clear advantages over real
39 antibodies for sensor applications: they are easy to fabricate, intrinsically stable, robust, and
40 are able to operate in extreme environments [1], [2] and [3]. MIPs could provide an
41 alternative, inexpensive, fast, and efficient diagnostic method for highly sensitive analytical
42 procedures within the pharmaceutical area [3].

43

44 When imprinting complex bio-macromolecules some of the most significant drawbacks in
45 MIP technology are the unprecedented degree of influence that the variation in pH [4], ionic
46 strength and local matrix effects all have on the gel properties [5], [6], [7] and [8]. This can
47 affect the three dimensional shape and chemical characteristics of the template molecule
48 during polymerisation. This is particularly true when imprinting large bio-macromolecules
49 such as proteins. Proteins are relatively labile, and have variable conformations which are
50 sensitive to solvent environments, pH and temperature, all of which present a variety of
51 challenges [5]. It has been thought that low imprinting capacities associated with bio-
52 macromolecules could be caused by the use of charged functional monomers causing non-
53 specific electrostatic interactions [5]. Moreover, as with antibodies, MIPs have also shown a
54 degree of cross-selectivity, in that they can bind molecules similar to the native template and
55 cause non-specific binding. It is thought that this is due in part to an excess of functional
56 monomer molecules being randomly distributed and frozen within the imprinted cavity
57 during polymerisation that have an affinity for non-template molecules [3] and [9]. Thus,
58 more sophisticated monomers capable of forming better, stronger and more stable

59 interactions that offer better positioning and complementary functionality are widely being
60 sought. Once these parameters are optimised, application to biosensors and analysis of actual
61 biological samples would be more realistic [6], [10], [11] and [12].

62

63 Biosensors for proteins are currently expensive to develop because they require the use of
64 expensive antibodies [3] and [13]. However, as MIPs are becoming more and more promising
65 as viable alternatives to natural receptors new MIP-based sensor strategies are being
66 developed [3]. The main advantage of biosensors is the ability to sample outside the
67 laboratory environment with minimal user input. One important part of bio-sensing is
68 transducers, which monitor the reaction between bio-selector and analyte. Among various
69 physical transducers (electrochemical, piezoelectric, etc.), mass sensitive devices such as
70 surface acoustic wave (SAW), surface plasmon resonance (SPR) and quartz crystal
71 microbalance (QCM) have become popular for sensing applications [14], [15], [16] and [17].

72

73 Following the thorough analysis of QCM systems for use in fluids over the past 2 decades,
74 this has allowed for more esoteric applications including bio-sensing [16]. In most cases
75 quartz resonators are integrated to oscillator circuits to form a QCM for micro weighing
76 applications. Normally, an equivalent circuit model is fitted to the impedance curve, and the
77 obtained parameters can be used for calculating the resonant frequency and dissipation (D) of
78 the quartz crystal i.e. mass and viscoelastic properties of the deposited layers [15] and [16].
79 Determining the impedance curve has many advantages; first and foremost it has expanded
80 the range of measurable parameters from rigid thin films, to biologically relevant films of
81 “soft” viscoelastic material. These QCM couplings have been widely used for biomaterials
82 and biosensor studies [10], [12], [16], [18] and [19], where surface confined bio-molecular

83 interactions have provided an insight into dissolution of polymer coatings, DNA
84 hybridisation, cell response to pharmacological substances, molecular interactions of drugs
85 and their delivery. The QCM has also been utilised as an immunosensor, where analytes are
86 recognised by antibodies, which are immobilised on a thin layer deposited on a crystal surface.
87 Resulting mass changes are transformed into an electronically measurable quantity. The
88 objective behind the majority of QCM research is to use sensor technology to develop a rapid
89 method for the measurement of bio-molecular affinity reactions, and an in-depth analysis of
90 electrochemical deposition, adsorption and reaction mechanisms of polymers coated on
91 electrodes as ‘thin films’ [10], [12], [18], [19] and [20].

92

93 The focus of this paper is the tailoring of QCM electrode surface chemistry (i.e. specialised
94 polymer coatings), with a view that these devices can discriminate proteins for bio-sensing
95 and basic surface-molecular interaction studies. In this work, we demonstrate the application
96 of the QCM technique to distinguish between the behaviour of MIPs and NIPs in the
97 presence of cognate and non-cognate proteins. Bovine haemoglobin (BHb, 64.5 kDa) was
98 chosen as a model protein for its well-known function in the vascular system as a carrier of
99 oxygen, also in aiding the transport of carbon dioxide and regulating blood pH [3] and [13].
100 Bovine serum albumin (BSA, 66 kDa), a non metalloprotein of similar molecular weight to
101 BHb, served to test the selectivity of the BHb-MIP to BSA compared to template BHb, and
102 was compared across a family of acrylamide-based polymer hydrogels.

103

104 2. Experimental

105 2.1. Materials

106

107 Acrylamide (AA), N-hydroxymethylacrylamide (NHMA), N-iso-propylacrylamide (NiPAm),
108 N,N'-methylenebisacrylamide (bis-AA), ammonium persulphate (APS), N,N,N',N'-
109 tetramethylethylenediamine (TEMED), sodium dodecyl-sulphate (SDS), glacial acetic acid
110 (AcOH), bovine haemoglobin (BHb), bovine serum albumin (BSA), hen egg-white lysozyme
111 (Lyz), thaumatin from *Thaumatococcus daniellii* (Thau), bovine pancreatic trypsin (Tryp) and
112 equine heart myoglobin (Mb) were all purchased from Sigma–Aldrich, Poole, Dorset, UK.
113 Sieves (75 μm) were purchased from Endecotts Ltd. and Inoxia Ltd., UK. AT-cut quartz
114 crystal pieces (9 MHz fundamental resonance) with gold-on-chrome electrodes were supplied
115 by Nihon Dempa Kogyo Company Ltd. (Tokyo, Japan).

116

117 2.2. HydroMIP preparations

118

119 Hydrogel MIPs were synthesised by separately dissolving AA (54 mg), NHMA (77 mg),
120 NiPAm (85.6 mg) and bis-AA as cross-linker (6 mg), (8.5 mg) and (9.5 mg), respectively
121 along with template protein (12 mg) in 960 μL of MilliQ water. The solutions were purged
122 with nitrogen for 5 min, followed by an addition of 20 μL of a 10% (w/v) APS solution and
123 20 μL of a 5% (v/v) TEMED solution. Polymerisation occurred at room temperature (RT, 22
124 ± 2 $^{\circ}\text{C}$) giving total gel densities (%T) of 6%T, AA/bis-AA (w/v); 8.5%T, NHMA/bis-AA
125 (w/v); 9.5%T, NiPAm/bis-AA (w/v), and final crosslinking densities (%C) of 10%C (9:1,
126 w/w) for all hydrogels.

127

128 For every MIP created a non-imprinted control polymer (NIP) was prepared in an identical
129 manner but in the absence of protein. After polymerisation, the gels were granulated
130 separately using a 75 μm sieve. Of the resulting gels, 500 mg were transferred into 1.5 mL
131 centrifuge Eppendorf tubes and conditioned by washing with five 1 mL volumes of MilliQ
132 water followed by five 1 mL volumes of 10% (w/v):10% (v/v) SDS:AcOH (pH 2.8) and
133 another five 1 mL volume washes of MilliQ water to remove any residual 10% (w/v):10%
134 (v/v) SDS:AcOH eluent and equilibrated the gels. Each wash step was followed by a
135 centrifugation, whereby the gels were centrifuged using an Eppendorf mini-spin plus
136 centrifuge for 3 min at 6000 rpm (RCF: $2419 \times g$). All supernatants were collected for
137 analysis by spectrophotometry to verify the extent of template removal. It should be noted
138 that the last water wash and eluent fractions were not observed to contain any protein.
139 Therefore we are confident that any remaining template protein within the MIPs did not
140 continue to leach out during the rebinding studies.

141

142 2.3. Rebinding studies

143

144 Once the gels (500 mg) were equilibrated, a 1 mL template protein solution prepared in
145 MilliQ water containing 3 mg of protein was added to the target MIPs and NIP controls and
146 was allowed to associate at RT (22 ± 2 °C) for 20 min. Selectivity studies were also
147 conducted to assess the relative imprinting factor of the original protein template. This was
148 achieved by loading non-cognate proteins on a BHb imprinted gel. Gels were then washed
149 with four 1 mL volumes of MilliQ water. Each reload and wash step for all MIPs and NIP
150 controls was followed by centrifugation at 6000 rpm (RCF: $2419 \times g$) for 3 min. All
151 supernatants were collected for analysis by spectrophotometry.

152

153 2.4. Spectrophotometric analysis

154

155 Calibration curves in MilliQ water and 10% (w/v):10% (v/v) SDS:AcOH were prepared for
156 BHB, BSA, Lyz, Tryp and Mb. Spectral scans revealed peak wavelengths for BHB in MilliQ
157 water and 10% (w/v):10% (v/v) SDS:AcOH to be 405 nm and 395 nm, respectively. Peak
158 wavelengths for BSA in MilliQ water and 10% (w/v):10% (v/v) SDS:AcOH were found to be
159 288 nm and 290 nm respectively. Peak wavelengths for Lyz in MilliQ water and 10%
160 AcOH:SDS were found to be 291 nm and 296 nm respectively. Peak wavelengths for Tryp in
161 MilliQ water and 10% (w/v):10% (v/v) SDS:AcOH were found to be 293 nm. Peak
162 wavelengths for Mb in MilliQ water, 10% (w/v):10% (v/v) SDS:AcOH were found to be 410
163 nm, and 396 nm respectively. Analysis and subsequent determination of protein
164 concentration in appropriate media was performed at specific peak wavelengths using a UV
165 mini-1240 CE spectrophotometer (Shimadzu Europa, Milton Keynes, UK).

166

167 2.5. Quartz crystal microbalance (QCM) analysis of thin film MIPs

168

169 QCM crystals were sealed and air capped (single-sided) with PVC glue in-order to prevent
170 short circuiting when the QCM was submerged in solution [10]. Poly AA, NHMA and
171 NiPAm gels for BHB were synthesised using the hydrogel production procedures outlined in
172 Section 2.2. Before polymerisation, MIPs and NIPs were deposited as thin films onto the
173 capped QCM crystals. Thin-films were achieved by beading and compressing 10 μ L of the
174 polymerising solutions directly onto the crystals. QCM frequency and impedance

175 measurements were taken using an Agilent 4194A Impedance Analyser. An in-house written
176 QBasic programme was used to drive the analyser and collect series resonance frequency and
177 impedance data in real time.

178

179 2.5.1. Elution and rebinding studies

180

181 MIP and NIP polyAA thin-film capped crystals were firstly immersed in MilliQ water,
182 followed by 10% (w/v):10% (v/v) SDS:AcOH in order to remove imprinted protein primarily
183 from the surface of the polymer. This was followed by another submersion in MilliQ water to
184 remove any residual surfactant and to re-condition the hydrogel. After subsequent
185 stabilisation of the QCM response, template protein was reloaded by immersing the QCM in
186 a 3 mg/mL BHb solution and the response trace was recorded at RT (22 ± 2 °C).

187

188 2.5.2. Selectivity studies

189

190 Continuous real-time scans were conducted in-order to assess characteristic impedance
191 changes of the gels during surface exposure to wash, elute and protein rebinding conditions.
192 During a typical run, the MIP thin-film capped crystals were submerged sequentially in
193 various solutions such as 10% (w/v):10% (v/v) SDS:AcOH, MilliQ water or 3 mg/mL protein
194 solutions (cognate BHb and non-cognate BSA, Thau, Lyz and Tryp) for a set time of 5 min
195 each, and crystal impedance and frequency responses were recorded at RT (22 ± 2 °C). The
196 latter procedure was followed for AA, NiPAm and NHMA based MIP hydrogels for BHb.

197

198 3. Results and discussion

199 3.1. MIP selectivity

200 The molecular imprinting effect is characterised by the rebinding capacity (Q) of protein to
201 the gel polymer (mg/g) exhibited by the protein-specific MIP and the control NIP, and is
202 calculated using Eq. (1), where C_i and C_r are the initial protein and the recovered protein
203 concentrations (mg/mL) respectively (which specifies the specific protein bound within the
204 gel), V is the volume of the initial solution (mL), and g is the mass of the gel polymers (g).

205

$$206 \quad Q = \frac{[C_i - C_r]V}{g} \quad (1)$$

207

208 Fig. 1A shows the rebinding capacities and imprinting factors of polyacrylamide (polyAA)
209 MIP and NIPs for several different proteins. The internal measure of the imprinting factor
210 between MIP and NIP serves to demonstrate that the MIP possesses selective cavities for the
211 rebinding of template molecule compared to NIP controls. It can clearly be seen that there is
212 a distinctive rebinding capacity variation for each imprinted protein template within a
213 polyAA MIP. This has previously been attributed to protein size, cross-linking density, and
214 the initial degree of association within the polymer matrix [4].

215 Gels based on N-hydroxymethylacrylamide (NHMA) exhibited similar rebinding trends,
216 whereas poly-N-isopropylacrylamide gels (polyNiPAm) demonstrated lower rebinding
217 capacities. Thus, bulk gel characterisation revealed the highest rebinding capacities for BHb
218 MIPs based on polyAA ($Q = 4.8 \pm 0.21$), followed by polyNHMA ($Q = 4.3 \pm 0.32$),

219 polyNiPAm ($Q = 3.6 \pm 0.45$). These gel imprinting trends are in agreement with those
220 previously published [4], [9] and [10].

221

222 Selectivity studies were also conducted to confirm a BHb specific imprinting effect and to
223 assess the relative imprinting factor of cross-selective binding profiles. The cross-reactivity of
224 the BHb-imprinted MIPs for non-cognate proteins was quantified using relative imprinting
225 factors (k), Eq. (2), where IF_{BHb} is the imprinting factor for BHb, and is calculated by $IF =$
226 $[C_i - C_r]MIP/[C_i - C_r]NIP$, and IF_x is the imprinting factor of the cross-reacting non-
227 cognate proteins on a BHb MIP. For the template BHb $k = 1$, and for non-cognate proteins
228 that are less-specific for the BHb MIP, $k < 1$.

229

$$230 \quad k = \frac{IF_{BHb}}{IF_x} \quad (2)$$

231 The data (Fig. 1B) suggests that both non-cognate trypsin (Tryp) and lysozyme (Lyz) proteins
232 have relatively low affinities for the BHb-specific MIP, $k \approx 0.2 \pm 0.05$. However, bovine
233 serum albumin (BSA), which is a similar size to BHb, exhibited a high degree of interference
234 binding (cross selectivity) resulting in high k values of 0.65 ± 0.05 . Myoglobin (Mb) also
235 exhibited some degree of cross-selectivity; this can be attributed to the size of Mb, which is a
236 quarter that of BHb (17.5 kDa), and its similarity to a single BHb sub-unit [4]. Interestingly
237 though, when reversed, a polyAA BSA-MIP exposed to non-target BHb protein had
238 relatively low affinity. It would appear that BSA has a high ability to bind non-specifically to
239 a BHb MIP, whereas BHb does not exhibit the same ability within a BSA MIP.

240

241 Competitive binding studies using a 50:50 mixture of BHb:BSA (3 mg/mL total) on a MIP-
242 BHb were also conducted (Fig. 1B). The addition of BSA caused an obvious capacity
243 decrease of BHb binding on the BHb-MIP, suggesting that the rebinding of BHb was
244 displaced by the competing BSA or by protein-protein interactions [21]. As the size,
245 structure, and specificity of the imprinted cavities should be in favour of the BHb template, it
246 is rational that the addition of BSA as a competing protein would not bind to the BHb-
247 specific imprinted cavities. Gai et al. previously demonstrated that BSA does not bind
248 specifically to a BHb MIP, but rather displaces the non-specific recognition sites of cavities
249 and the nonspecific binding of BHb to BHb-MIP [21]. Moreover, although BSA and BHb
250 share similar sizes (66 kDa and 64.5 kDa, respectively), it should be noted that BSA has a pI
251 of 4.6 and BHb a pI of (6.8–7.0). Since competitive binding was performed under MilliQ
252 water (pH 5.4), conditions are in favour of BSA [21] and [22]. Above its pI, BSA becomes
253 negatively charged and the groups exist as single bondNH₂ and single bondCOO⁻, this
254 overall negative net charge induces more favourable and complementary hydrogen bonding
255 interactions, resulting in increased specific as well as non-specific binding [4].

256

257 3.2. QCM sensor application of MIPs

258 Thin film BHb MIPs were prepared on the surface of a QCM chip and the sensor was
259 exposed sequentially to MilliQ water, 10% (w/v):10% (v/v) SDS:AcOH and 3 mg/mL protein
260 solutions at RT (22 ± 2 °C). We have previously published on the thickness of the thin films
261 on sensor chips with an average thickness of 138 ± 9 nm [6]. Given that for a 9 MHz crystal
262 the shear wave decay length is 250 nm at RT [23], we are within the sensing region of the
263 QCM to measure both bulk and surface effects within the MIP film.

264

265 Fig. 2A and B shows the QCM impedance and frequency responses following immersion in a
266 solution of 10% (w/v):10% (v/v) SDS:AcOH in order to remove imprinted protein from the
267 surface of the polymer. Previous investigations have shown that optimum conditions for
268 protein removal of up to 80% have been achieved using 10% (w/v):10% (v/v) SDS:AcOH
269 [9]. Using this acid/surfactant combination the positively charged protein attaches to the
270 negatively charged surface of SDS micelles and disrupts the hydrophobic bonds. Since there
271 is a significant shift in both resonance frequency and impedance it can be assumed that some
272 of the BHb imprinted template has been successfully removed from the MIP.

273 It is worth noting the two distinct differences in the impedance response when compared with
274 the frequency response. Firstly, the impedance response has much reduced noise in the signal
275 in contrast to the frequency response. Secondly, there are significant additional transitions
276 (e.g. at 350 and 650 s) in the signal which are being observed in the Z response, but not in the
277 frequency response. It has been suggested that whereas the frequency response predominately
278 demonstrates the QCM mass response only within an adlayer, the electrical impedance gives
279 a combination response of the mass effect as well as subsequent changes in the viscoelasticity
280 of the adlayer possibly due to molecular relaxations within the adsorbed layer over a longer
281 timescale following initial immersion [23], [24] and [25].

282

283 After subsequent stabilisation of the QCM response, the template BHb was then reloaded by
284 immersing the QCM in a 3 mg/mL BHb solution and the response trace recorded. Fig. 2C and
285 D compares the final QCM impedance and frequency responses to template BHb exposure of
286 each MIP and its corresponding NIP. It can be seen that upon addition of a 3 mg/mL BHb
287 solution to the BHb MIP caused significant QCM responses compared with NIP thin-film
288 hydrogels. This suggests that MIP thin-film gels are affected by specific binding of target

289 BHb. This distinct difference between responses exhibited by MIP and the NIP control
290 strongly supports that binding and elution of target protein gave rise to distinct impedance
291 transitions. The 200 ± 50 Hz frequency shift observable by both MIP and NIP during the
292 initial loading step (Fig. 2D) is suggestive of a solution viscosity effect.

293

294 Real time impedance response following sequential immersion in solutions of BHb, 10%
295 (w/v):10% (v/v) SDS:AcOH and BSA were also measured. Three distinct types of responses
296 were observed depending on the acrylamide-based monomer used. The key difference
297 between the polymers is their hydrophilicity dictated by the hydrophilic hydroxyl group in
298 NHMA and the hydrophobic isopropyl group in NiPAm. AA sits between the two in degree
299 of hydrophilicity (polyNHMA > polyAA > polyNiPAm), which agrees with the order of best
300 performance of the polymers as BHb MIPs in previous QCM studies [10]. Fig. 3 compares
301 the final QCM response to cognate and non-cognate protein exposure of each MIP with its
302 corresponding NIP. Interestingly, the NiPAm MIP and NIP both show a near zero frequency
303 response to template BHb and non-cognate BSA, indicating that NiPAm is equally
304 unselective for both proteins as is the control non-imprinted polymer. The non-response of
305 NiPAm to either BHb or BSA suggests that there is a resistance to either protein to bind to
306 the polymer. The striking difference in selectivities between cognate and non-cognate
307 proteins for NHMA and AA suggests that the hydroxyl group in NHMA plays a significant
308 role in the selective binding of BHb and the lack of binding of BSA.

309 Moreover, variations of the series resonance frequency demonstrated to be highly dependent
310 on the test solution used (Fig. 4A). The impedance data is presented here because in
311 comparison to the frequency response, there is much reduced noise in the signal following
312 each solution phase immersion. It can be seen that MIP thin-films exposed to a 10%:10%

313 (v/v) SDS:AcOH solution exhibited an immediate significant decrease in impedance ($500 \pm$
314 100Ω); this is possibly due to the increase in the viscosity of the solution caused by the
315 presence of SDS micelles in the solution. Moreover, it can clearly be seen that the
316 introduction of non-template BSA also exhibits an impedance response within the poly AA
317 MIP, suggesting some non-specific binding within the BHb-HydroMIP. Thus, there is a high
318 degree of cross-selectivity present for our AA-based MIPs ($>70\%$), and this interference is
319 absent when NHMA-based MIPs are used ($<20\%$) as seen in Fig. 3.

320 To further test the BHb-MIP selectivity, we investigated the rebinding of template BHb after
321 exposing the MIP with non-target BSA. The resulting quantified imprinting effect of BHb for
322 polyAA MIP thin-film gels can be seen in the impedance responses (Fig. 4B). The
323 comparison demonstrates that both HydroMIP and HydroNIP films act differently under
324 water wash, elution and load (solution immersion) treatments following BSA loading. It can
325 be seen that when non-target BSA is loaded first, the QCM impedance response is now
326 negligible. Interestingly, impedance responses are also almost negligible when BHb is
327 introduced after prior exposure to BSA. Although the loaded BSA did not associate
328 specifically with the BHb-MIP thin-film surface, an interesting and lasting effect inhibits
329 BHb from easily binding to recognition sites. Indeed, BSA is similar to the template BHb in
330 size, but the spatial arrangement of the effective groups on its exterior are different from
331 BHb, and the recognition sites in the BHb-MIP cavities are not complementary in shape to
332 BSA [22]. Therefore, little to no selectivity of BSA on BHb-MIPs should be expected.
333 Therefore, in the case of AA-based MIPs, the inhibition effect is most likely due to the ability
334 of BSA to exhibit protein binding on the MIP surface but not within cavities. Formation of a
335 BSA biolayer above (but not within) the cavities would block subsequent cavity-selective
336 MIP binding for its cognate protein [22]. This is further indication that BHb-MIPs distinguish
337 proteins not only based on molecular size, but also on the synergistic effect of shape memory,

338 and multiple weak hydrogen bonding interactions specific to template protein in
339 macromolecular recognition [21], [22] and [26].

340

341 Moreover, further studies to interrogate the recognition capabilities of MIPs were carried out
342 using a range of non-metalloproteins chosen for their different sizes and functionalities
343 compared to BHb, BSA and Mb. Of these proteins: lysozyme (Lyz), a glycoside hydrolase
344 enzyme (14.7 kDa) that is part of the innate immune system, and exists as a natural form of
345 protection from pathogens like Salmonella, E. coli, and Pseudomonas [9], [10] and [27].
346 Thaumatin (Thau), a sweetener or flavour modifier (22 kDa) often used in crystallisation
347 studies due to its ease of use and crystal formation [27]. Trypsin (Tryp), a serine protease
348 enzyme or proteinase 'digestive enzyme' (23.8 kDa) commonly imprinted within MIPs [9],
349 [10] and [27]. Fig. 5 shows that the BHb-MIPs based on all three polymers (AA, NHMA, and
350 NiPAm) are essentially non-responsive to the addition of the three smaller proteins Thau, Lyz
351 and Tryp respectively. An average NIP response was calculated based on all three polymers
352 and used as an illustration to demonstrate the negligible responses exhibited by the MIP
353 properties. The negligible responses exhibited by the QCM sensor concur with the qualitative
354 data and confirm that these small proteins exhibit no selective specific/non-specific binding
355 characteristics to a BHb-imprinted MIP.

356

357 4. Conclusions

358 A family of acrylamide-based MIPs have been characterised for their imprint efficiency using
359 spectrophotometric and QCM sensor techniques for biosensor development. Varied rebinding
360 capacities and relative imprinting factors have been achieved using bulk characterisation. We

361 have demonstrated that MIP selectivity is a function of the hydrophilicity of the acrylamide
362 monomer used to form the MIP. Three distinct types of QCM responses were observed
363 depending on the acrylamide used (polyNHMA > polyAA > polyNiPAm), which agrees with
364 the order of best performance of the polymers in previously published QCM studies. The
365 selectivity of BHb-MIP for BHb and BSA was also compared via QCM, along with several
366 other proteins. Results demonstrated BHb-MIP to have better selective adsorption and
367 recognition properties to BHb than BSA when using the hydrophilic NHMA as a MIP
368 polymer matrix. Therefore, the QCM sensor was able to indicate MIP surface activity and
369 provide physical interpretation in terms of hydrophilicity of the polymer matrix that forms the
370 MIP and protein selectivity. Our QCM sensor also has the ability to assess the extent of
371 specific protein binding by sensing surface-specific bound cognate protein to MIPs compared
372 to non-imprint NIP controls. We expect, once fully developed, that the benefits of sensitivity,
373 specificity and stability of MIPs coupled with discriminatory techniques, such as QCM, will
374 be crucial to the future impact of portable diagnostics for personal healthcare and use by
375 health professionals. The technology also presents major potential benefits to environmental
376 and food monitoring.

377

378 Acknowledgements

379 The authors wish to thank the UK Engineering and Physical Sciences Research Council
380 (EPSRC) Grants (EP/G014299/1) and NERC/ACTF (RSC) for supporting this work.

381

382 References

383 [1] S. Pradhan, M. Boopathi, O. Kumar, A. Baghel, P. Pandey, T.H. Mahato, B. Singh, R.
384 Vijayaraghavan, Molecularly imprinted nanopatterns for the recognition of biological warfare
385 agent ricin *Biosens. Bioelectron.*, 25 (2009), pp. 592–598

386 [2] D.R. Kryscio, N.A. Peppas Critical review and perspective of macromolecularly
387 imprinted polymers *Acta Biomater.*, 8 (2012), pp. 461–473

388 [3] M.J. Whitcombe, I. Chianella, L. Larcombe, S.A. Piletsky, J. Noble, R. Porter, A. Horgan
389 The rational development of molecularly imprinted polymer-based sensors for protein
390 detection *Chem. Soc. Rev.*, 40 (2011), pp. 1547–1571

391 [4] H.F. El-Sharif, Q.T. Phan, S.M. Reddy Enhanced selectivity of hydrogel-based
392 molecularly imprinted polymers (HydroMIPs) following buffer conditioning *Anal. Chim.*
393 *Acta*, 809 (2014), pp. 155–161

394 [5] E. Verheyen, J.P. Schillemans, M. van Wijk, M. Demeniex, W.E. Hennink, C.F. van
395 Nostrum Challenges for the effective molecular imprinting of proteins *Biomaterials*, 32
396 (2011), pp. 3008–3020

397 [6] S.M. Reddy, D.M. Hawkins, Q.T. Phan, D. Stevenson, K. Warriner Protein detection
398 using hydrogel-based molecularly imprinted polymers integrated with dual polarisation
399 interferometry *Sens. Actuators B: Chem.*, 176 (2013), pp. 190–197

400 [7] S.A. Piletsky, N.W. Turner, P. Laitenberger Molecularly imprinted polymers in clinical
401 diagnostics – future potential and existing problems *Med. Eng. Phys.*, 28 (2006), pp. 971–977

402 [8] M.E. Byrne, V. Salián Molecular imprinting within hydrogels. II. Progress and analysis
403 of the field *Int. J. Pharm.*, 364 (2008), pp. 188–212

404

405 [9] D.M. Hawkins, D. Stevenson, S.M. Reddy Investigation of protein imprinting in
406 hydrogel-based molecularly imprinted polymers (HydroMIPs) *Anal. Chim. Acta*, 542 (2005),
407 pp. 61–65
408

409 [10] S.M. Reddy, Q.T. Phan, H. El-Sharif, L. Govada, D. Stevenson, N.E. Chayen
410 Protein crystallization and biosensor applications of hydrogel-based molecularly imprinted
411 polymers *Biomacromolecules*, 13 (2012), pp. 3959–3965

412 [11] P.A. Lieberzeit, R. Samardzic, K. Kotova, M. Hussain MIP sensors on the way to
413 biotech application: selectivity and ruggedness *Proc. Eng.*, 47 (2012), pp. 534–537

414 [12] B.B. Prasad, I. Pandey Molecularly imprinted polymer-based piezoelectric sensor for
415 enantio-selective analysis of malic acid isomers *Sens. Actuators B: Chem.*, 181 (2013), pp.
416 596–604

417 [13] S.M. Reddy, G. Sette, Q. Phan Electrochemical probing of selective haemoglobin
418 binding in hydrogel-based molecularly imprinted polymers *Electrochim. Acta*, 56 (2011), pp.
419 9203–9208

420 [14] G.N.M. Ferreira, A. da-Silva, B. Tomé Acoustic wave biosensors: physical models and
421 biological applications of quartz crystal microbalance *Trends Biotechnol.*, 27 (2009), pp.
422 689–697

423 [15] T.M.A. Gronewold Surface acoustic wave sensors in the bioanalytical field: recent
424 trends and challenges *Anal. Chim. Acta*, 603 (2007), pp. 119–128
425

426 [16] U. Latif, S. Can, O. Hayden, P. Grillberger, F.L. Dickert Sauerbrey and anti-Sauerbrey
427 behavioral studies in QCM sensors – detection of bioanalytes *Sens. Actuators B: Chem.*, 176
428 (2013), pp. 825–830

429 [17] C. Steinem, A. Janshoff *Sensors: piezoelectric resonators* P. Worsfold, A. Townshend,
430 C. Poole (Eds.), *Encyclopedia of Analytical Science* (2nd ed.), Elsevier, Oxford (2005), pp.
431 269–276

432 [18] K.K. Reddy, K.V. Gobi Artificial molecular recognition material based biosensor for
433 creatinine by electrochemical impedance analysis *Sens. Actuators B: Chem.*, 183 (2013), pp.
434 356–363.

435 [19] K. Reimhult, K. Yoshimatsu, K. Risveden, S. Chen, L. Ye, A. Krozer
436 Characterization of QCM sensor surfaces coated with molecularly imprinted nanoparticles
437 *Biosens. Bioelectron.*, 23 (2008), pp. 1908–1914

438 [20] B. Khadro, C. Sanglar, A. Bonhomme, A. Errachid, N. Jaffrezic-Renault
439 Molecularly imprinted polymers (MIP) based electrochemical sensor for detection of urea
440 and creatinine *Proc. Eng.*, 5 (2010), pp. 371–374

441 [21] Q. Gai, F. Qu, T. Zhang, Y. Zhang The preparation of bovine serum albumin surface-
442 imprinted superparamagnetic polymer with the assistance of basic functional monomer its
443 application for protein separation *J. Chromatogr. A*, 1218 (2011), pp. 3489–3495

444 [22] Q. Gai, F. Qu, Y. Zhang The preparation of BHB-molecularly imprinted gel polymers
445 and its selectivity comparison to BHB and BSA *Sep. Sci. Technol.*, 45 (2010), pp. 2394–2399
446

447 View Record in Scopus | Full Text via CrossRef | Citing articles (9)

448 [23] K.A. Marx Quartz crystal microbalance: a useful tool for studying thin polymer films and
449 complex biomolecular systems at the solution–surface interface

450 *Biomacromolecules*, 4 (2003), pp. 1099–1120

451 [24] S. Kurosawa, J. Park, H. Aizawa, S. Wakida, H. Tao, K. Ishihara Quartz crystal
452 microbalance immunosensors for environmental monitoring *Biosens. Bioelectron.*, 22 (2006),
453 pp. 473–481

454 [25] T. Zhou, K.A. Marx, M. Warren, H. Schulze, S.J. Braunhut

455 The quartz crystal microbalance as a continuous monitoring tool for the study of endothelial
456 cell surface attachment and growth *Biotechnol. Prog.*, 16 (2000), pp. 268–277

457 [26] Zhou Xue, He Xi-Wen, Chen Lang-Xing, Li Wen-You, Zhang Yu-Kui

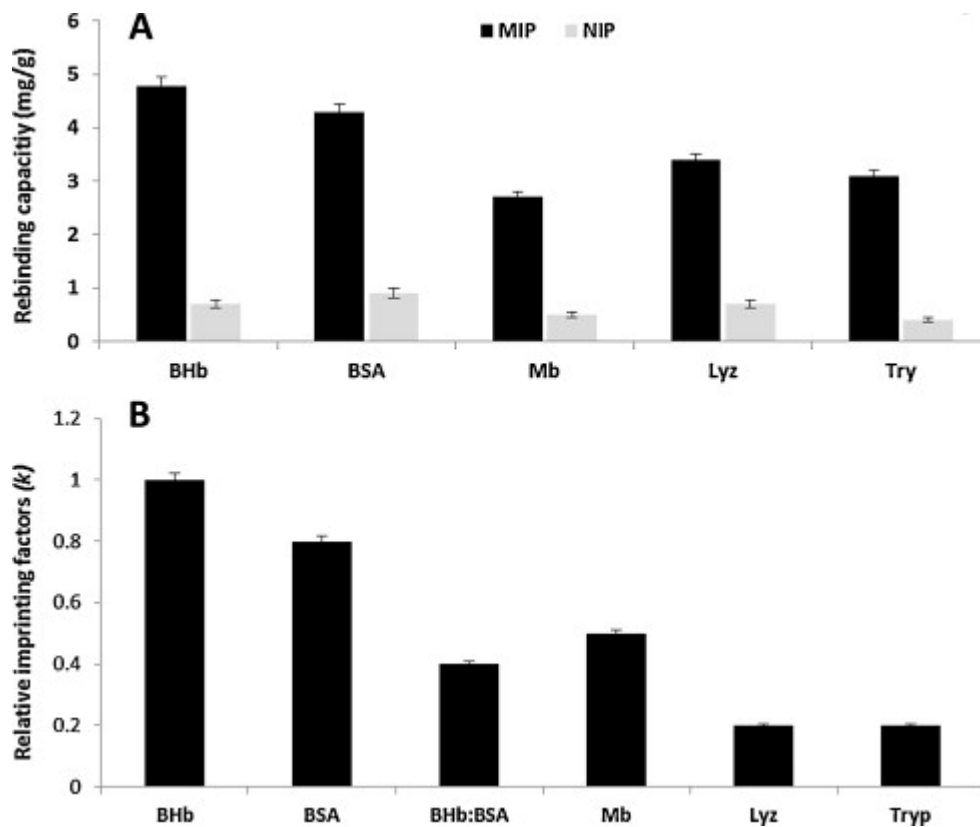
458 Optimum conditions of separation selectivity based on molecularly imprinted polymers of
459 bovine serum albumin formed on surface of aminosilica *Chin. J. Anal. Chem.*, 37 (2009), pp.
460 174–180

461 [27] E. Saridakis, S. Khurshid, L. Govada, Q. Phan, D. Hawkins, G.V. Crichlow, E. Lolis,
462 S.M. Reddy, N.E. Chayen Protein crystallization facilitated by molecularly imprinted
463 polymers *Proc. Natl. Acad. Sci.*, 108 (2011), pp. 11081–11086

464

465 Fig. 1.

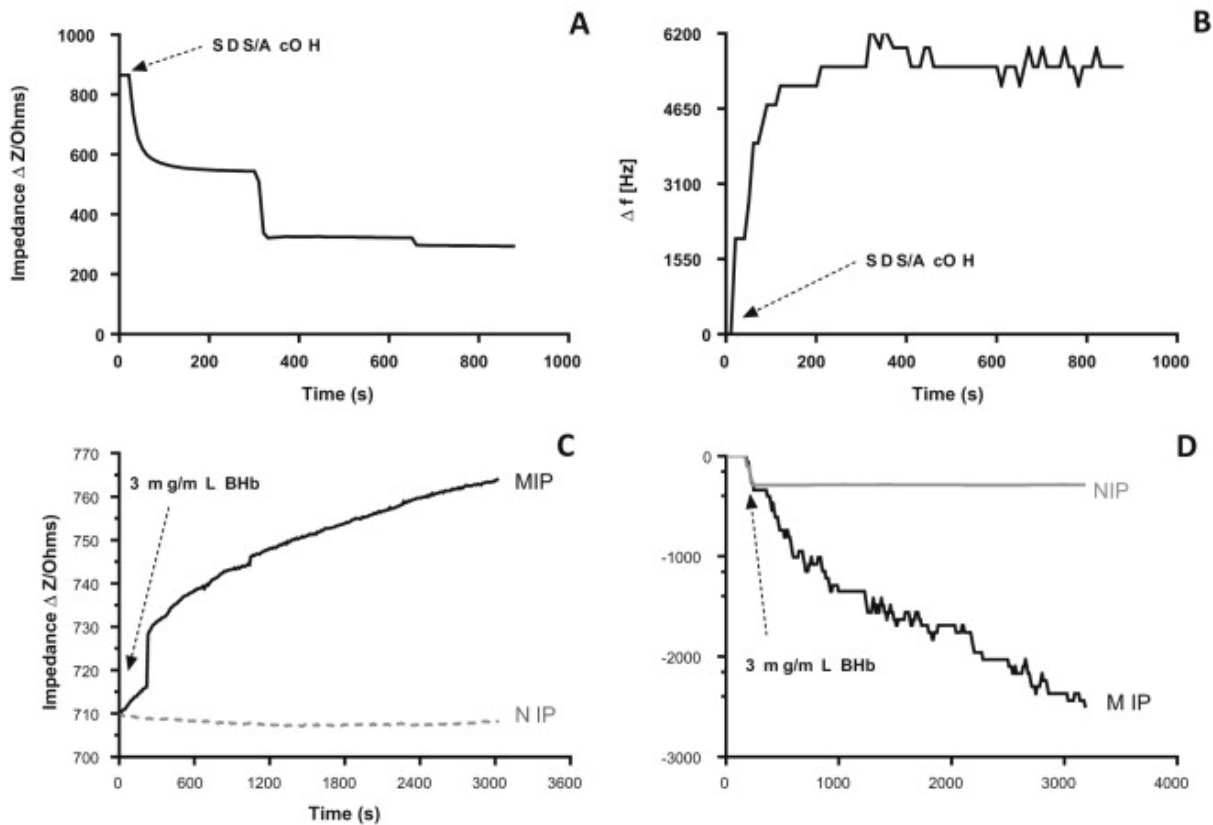
466 (A) Rebinding capacities (Q) and imprinting factors of MIP_{polyAA} and NIP_{polyAA} hydrogels for several
467 proteins in MilliQ water media: bovine haemoglobin (BHb), bovine serum albumin (BSA), myoglobin
468 (Mb), lysozyme (Lyz), trypsin (Tryp); (B) relative imprinting factors (k) for a range of BHb-
469 MIP_{polyAA} cross-reactants in MilliQ water media. Results illustrate higher MIP selectivities for cognate
470 BHb and the degree of cross-selectivity for other non-template analytes. Data represents
471 mean \pm S.E.M., $n = 3$.
472



473

474 Fig. 2.

475 QCM response to the immersion of polyAA-BHb hydrogel thin-film MIP in 10% (w/v):10% (v/v)
476 SDS:AcOH in order to follow protein elution (arrow indicates time of MIP immersion): (A) impedance
477 (ΔZ), (B) frequency (Δf); QCM responses to BHb (3 mg/mL) loading onto a BHb imprinted polyAA
478 hydrogel thin-film (arrow indicates time of immersion in protein solution): (C) impedance (ΔZ) and (D)
479 frequency (Δf).
480



481

482

483 Fig. 3.

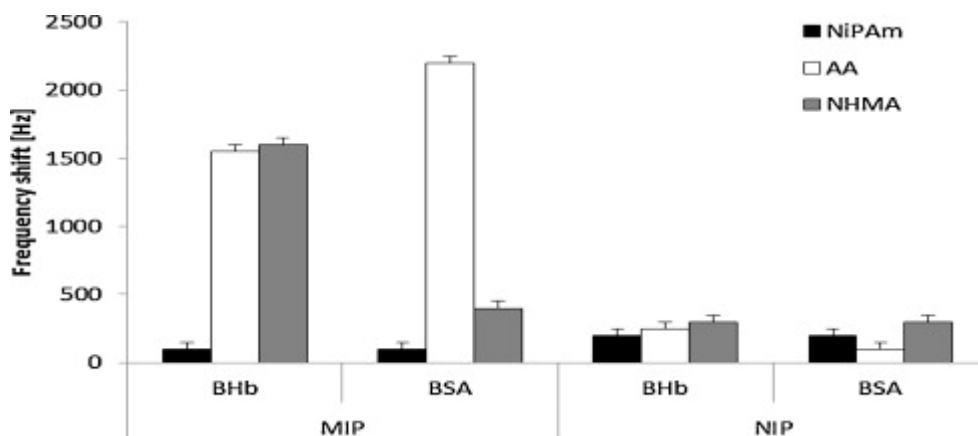
484 QCM frequency shift responses of NiPAM, AA and NHMA polymer MIPs and NIPs to cognate BHB

485 and non-cognate BSA loading (3 mg/mL) after 5 min of exposure. Data represents

486 mean \pm S.E.M., $n = 3$.

487

488



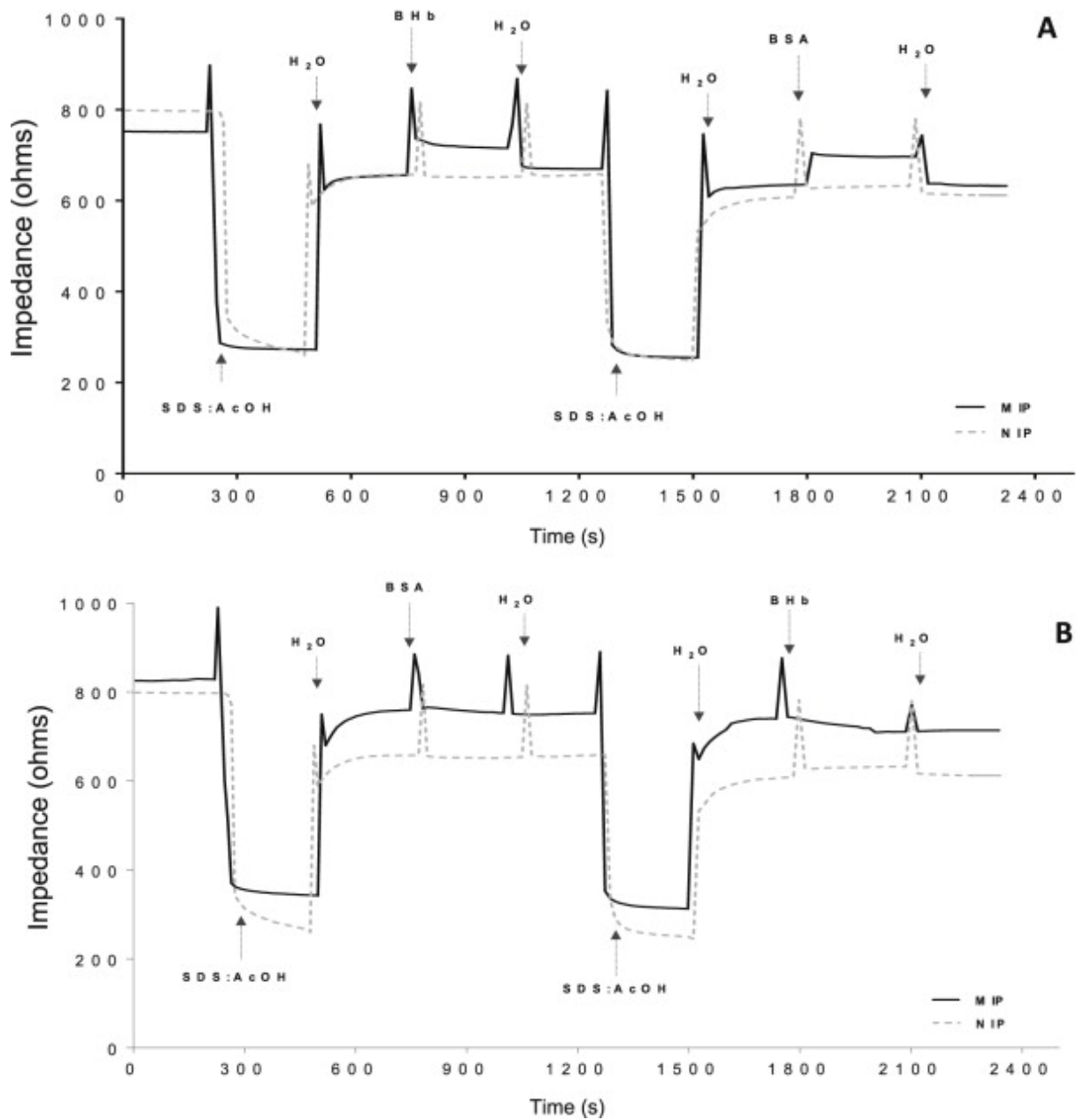
489

490 Fig. 4.

491 Real time QCM impedance responses: (A) direct BHB rebinding and BSA cross-selectivity on a BHB-

492 MIP_{polyAA}; (B) BSA cross-selectivity on a BHB-MIP_{polyAA} followed by BHB rebinding.

493



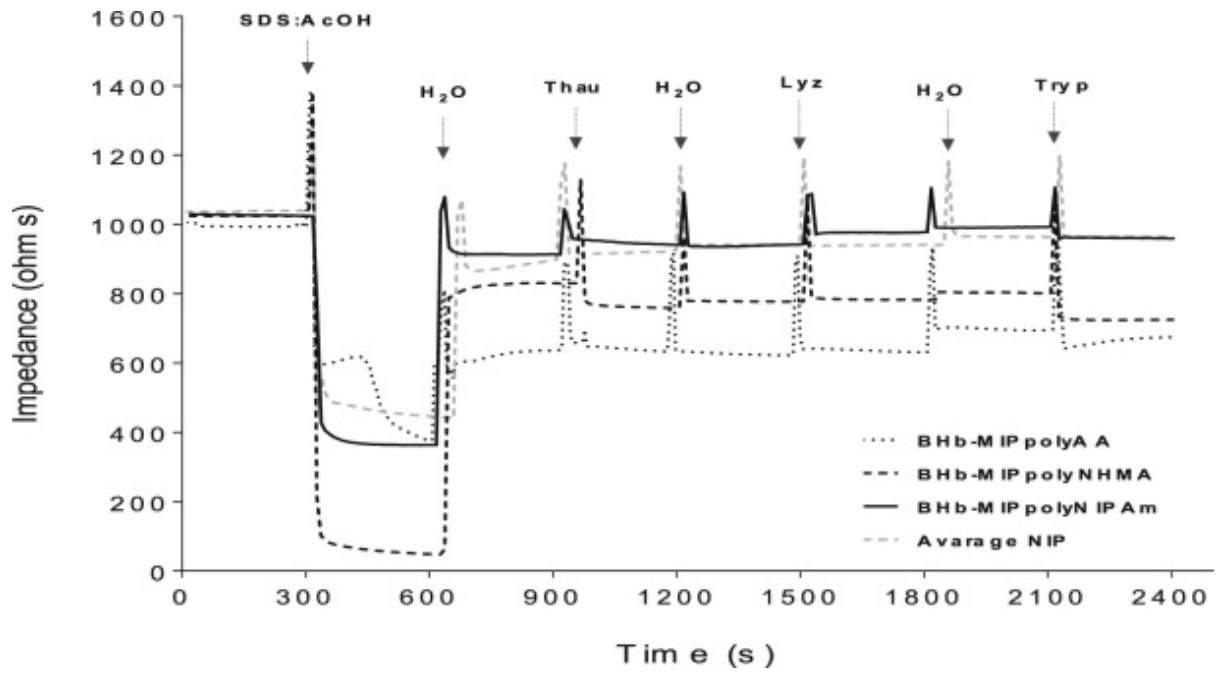
494

495

496 Fig. 5.

497 QCM response of functionalised acrylamide BHB MIPs to non-cognate proteins thaumatin (Thau),
 498 lysozyme (Lyz), and trypsin (Tryp) after H₂O washes and an SDS:AcOH elute.

499



500

501

502

503

504

505

506

507

508